

# Thiol-Specific Cross-Linkers of Variable Length Reveal a Similar Separation of SH1 and SH2 in Myosin Subfragment 1 in the Presence and Absence of MgADP<sup>†</sup>

Werner Kliche,\*<sup>‡</sup> Jens Pfannstiel,<sup>‡</sup> Markus Tiepold,<sup>‡</sup> Stanka Stoeva,<sup>§</sup> and Heinz Faulstich\*<sup>‡</sup>

Max-Planck-Institut für Medizinische Forschung, Jahnstrasse 29, D-69120 Heidelberg, Germany, and Physiologisch-Chemisches Institut der Universität Tübingen, Abteilung für Physikalische Biochemie, Hoppe-Seyler-Strasse 1, D-72076 Tübingen, Germany

Received March 17, 1999; Revised Manuscript Received May 18, 1999

**ABSTRACT:** A series of thiol-specific cross-linking reagents were prepared for studying the kinetics of cross-linking between SH1 (Cys<sub>707</sub>) and SH2 (Cys<sub>697</sub>) in rabbit skeletal muscle myosin subfragment 1. The reagents were of the type RSS(CH<sub>2</sub>)<sub>n</sub>SSR, with R = 3-carboxy-4-nitrophenyl and *n* = 3, 6, 7, 8, 9, 10, and 12, spanning distances from 9 to 20 Å. The reactions were monitored spectrophotometrically by measuring the release of 2-nitro-5-thiobenzoate. Reaction rates for modification of SH1 (*k*<sub>1</sub>) and for cross-linking (*k*<sub>2</sub>) were measured by the decrease of the K<sup>+</sup>(EDTA)-ATPase activity and the decrease of the Ca<sup>2+</sup>-ATPase activity, respectively, and corrected for the different reactivities of C<sub>n</sub>. Cross-linking rates in the presence and absence of MgADP showed similar dependence on the length of the reagents: While the cross-linking rates for *n* = 3 or *n* = 6 were close to those for *n* = 0 (Ellman's reagent), those for *n* = 7 and 8 were significantly increased. Thus the distance between SH1 and SH2 appears to be equal in both states and can be estimated as ≥15 Å, based on the length of the reagent with *n* = 8 in stretched conformation. Under rigor conditions, reactivity of SH1 differed significantly from that in the presence of MgADP, presumably because of shielding through a lipophilic domain. Similarly, the cross-linking rates *k*<sub>2</sub> for C<sub>3</sub>, C<sub>6</sub>, and C<sub>7</sub> in the absence of MgADP were ca. 15 times lower than in the presence of MgADP, suggesting a change in the structure of the SH2 region that depends on nucleotide binding. The results are discussed in terms of recent X-ray structures of S1 and S1–MgADP [Rayment et al. (1993) *Science* 261, 50–58; Gulick et al. (1997) *Biochemistry* 36, 11619–11628].

Muscle generates force by cyclic interactions between actin filaments and the head part of myosin at the expense of the chemical energy of ATP. Chymotryptic digestion of myosin produces subfragment 1 (S1),<sup>1</sup> containing the head region with the binding sites for ATP and actin and having one light chain (A1 or A2) bound. Further digestion of S1 with trypsin breaks S1 into three pieces, the 25, 50, and 20 kDa fragments. The 20 kDa fragment contains the two reactive thiols, Cys<sub>707</sub> (SH1) and Cys<sub>697</sub> (SH2). According to a recent X-ray structure of chicken S1 the two thiols are part of two

short α-helices connected by a kink at the conserved Gly<sub>699</sub> residue with a distance between SH1 and SH2 of about 17 Å (1). A similar value was found for the distance<sup>2</sup> between Thr<sub>688</sub> and Cys<sub>678</sub>, the two amino acids in *Dictyostelium discoideum* myosin II corresponding to Cys<sub>707</sub> and Cys<sub>697</sub> in chicken S1, and between Cys<sub>707</sub> and Cys<sub>717</sub> in smooth muscle S1. This distance was independent of the kind of ligand bound to S1 (2–6).

The region containing the two essential SH groups is of particular interest for studying movements, or the structural elements involved in them, that occur in the myosin head during force generation. The rotating lever arm hypothesis postulates the existence of a fulcrum point located close to the SH1 region (7–10), a proposition that was substantiated by the structure determination of the motor domain of smooth muscle myosin (6). In mutants of *Dictyostelium* myosin II, some replacements in the SH1/SH2 region caused dramatic functional defects (11, 12). Although SH1 and SH2 are not part of the active site, their chemical modification strongly

<sup>†</sup> Supported by the Deutsche Forschungsgemeinschaft (DFG).

\* To whom correspondence should be addressed: tel, (+49) 06203-106-257 (260); fax, (+49) 06203-106-259; e-mail, hfaulst@zellbio.mpg.de or wkliche@zellbio.mpg.de.

<sup>‡</sup> Max-Planck-Institut für Medizinische Forschung.

<sup>§</sup> Physiologisch-Chemisches Institut der Universität Tübingen.

<sup>1</sup> Abbreviations: A1 and A2, myosin alkali light chain 1 and 2; ArSS–(CH<sub>2</sub>)<sub>n</sub>–SSAr (C<sub>n</sub>, *n* = 3, 6, 7, 8, 9, 10, 12), alkylenebis(5,5'-dithio-2-nitrobenzoic acid); ArSSAr (C<sub>0</sub>, Ellman's reagent), 5,5'-dithiobis(2-nitrobenzoic acid); DACM, *N*-[7-(dimethylamino)-4-methyl-3-coumarinyl]maleimide; *k*<sub>1</sub>, rate constant for activation of the Ca<sup>2+</sup>-induced ATPase activity or inactivation of the K<sup>+</sup>(EDTA)-induced ATPase activity; *k*<sub>2</sub>, rate constant for inactivation of the Ca<sup>2+</sup>-induced ATPase activity; *k*<sub>2</sub>/*k*<sub>1</sub>, normalized cross-linking rate of SH1 and SH2; *k*<sub>A</sub> or *k*', pseudo-first-order rate constants for the reactions with Cys<sub>374</sub> in G-actin or the reaction with cysteine; NEM, *N*-ethylmaleimide; NTB<sup>−</sup>, 2-nitro-5-thiobenzoate; pPDM, *N,N'*-*p*-phenylenedimaleimide; SH1 and SH2, Cys<sub>707</sub> and Cys<sub>697</sub> of the S1 heavy chain; SH<sub>LC</sub>, reactive Cys of the A2 light chain; S1, myosin subfragment 1; S1A2, myosin subfragment 1 with the A2 light chain bound; S1A2–C<sub>n</sub>, S1A2 with SH1 reacted with one end of C<sub>n</sub>; S1A2=C<sub>n</sub>, S1A2 cross-linked between SH1 and SH2.

<sup>2</sup> The distance was calculated from the C<sub>α</sub> atom of Cys<sub>697</sub> in chicken S1 (Cys<sub>678</sub> in *Dictyostelium* S1; Cys<sub>707</sub> in smooth muscle S1) to the C<sub>α</sub> atom of Cys<sub>707</sub> (Thr<sub>688</sub> in *Dictyostelium* S1; Cys<sub>717</sub> in smooth muscle S1) complexed with various ligands with the program Ramol (Glaxo Wellcome, Edinburgh) using the Brookhaven Protein Data Bank files 2MYS (SO<sub>4</sub><sup>2−</sup>, chicken S1), 1BR1 and 1BR4 (MgADP·AlF<sub>4</sub> and MgADP·BeF<sub>3</sub>, smooth muscle S1), and 1MMD (MgADP·BeF<sub>3</sub>), 1MND (MgADP·AlF<sub>4</sub><sup>−</sup>), 1MNE (MgPPi), 1VOM (MgADP·VO<sub>4</sub>), 1MMA (MgADP), 1MMG (MgATPγS), and 1IMN (MgAMPPNP) (all *Dictyostelium* S1).

affected ATPase activity. Blocking of the most reactive SH1 inhibited  $K^+$ (EDTA)-ATPase but enhanced  $Ca^{2+}$ -ATPase (13, 14). Subsequent modification of the less reactive SH2 led to the loss of all ATPase activities (15–17). Cross-linking experiments suggested that conformational changes in the thiol region are likely to occur upon nucleotide binding (18–20).

A cross-linking reagent that is able to react with the two exposed thiols in myosin S1 in the presence as well as in the absence of MgADP is *p*-phenylenedimaleimide (pPDM) (21). On the basis of the dimensions of the pPDM molecule, the distance between SH1 and SH2 was found to be  $\geq 12$ –14 Å in the absence of MgADP. In the presence of MgADP, even a disulfide bond can be formed between SH1 and SH2 with Ellman's reagent (22, 23), showing that the two thiols can approach as close as 2 Å, a value that does not necessarily correspond to the average separation of the two thiols under these conditions. Important is not only the possibility of the reaction with a cross-linker of given length but also the kinetics of the cross-linking reaction, which in the case of Ellman's reagent was indeed rather slow. By both cross-linking reactions, with pPDM as well as with Ellman's reagent, MgADP was stably trapped within the active site (22, 24, 25).

In the present study we prepared a series of seven homologous cross-linking reagents  $C_n$  (8.6–20.3 Å), which react with thiols via a disulfide exchange reaction driven by the release of 2-nitro-5-thiobenzoate (NTB<sup>−</sup>), as in Ellman's reaction. Through the use of these reagents we aimed to identify, from the kinetics of the cross-linking reaction, the reagent with the best fit to the distance between SH1 and SH2. Intrinsic reactivity properties of the various reagents were considered by correcting the rate constants for cross-linking in a way similar to that proposed by Reisler and co-workers (26, 27). In addition to measuring the distance between the two thiols, we were interested in identifying changes in the environment of SH1 and SH2 induced by nucleotide binding.

## MATERIALS AND METHODS

**Protein Purification.** Myosin was prepared from rabbit skeletal muscle (28) and stored in 50% glycerol at  $-20^\circ\text{C}$ . Myosin subfragment 1 (S1) was prepared by digestion with  $\alpha$ -chymotrypsin (Serva) of soluble myosin (29), frozen in liquid nitrogen, and stored at  $-70^\circ\text{C}$ . In this study only the S1A2 isoform was used. A molecular weight of 115 000 (30) was assumed for S1A2. Protein concentrations of unmodified S1 were determined by measuring the absorbance at 280 nm [ $A_{280\text{nm}}^{1\%} = 7.5\text{ cm}^{-1}$  (31)]. The protein concentration of modified S1A2 was determined by the method of Bradford (32), using a calibration curve made with S1A2. Actin was prepared from rabbit muscle as described by Spudich and Watt (33). Actin concentrations were determined by measuring the absorbance at 290 nm using  $\epsilon_{290} = 26\,460\text{ M}^{-1}\text{ cm}^{-1}$  (34).

Actin was labeled with pyrenemaleimide (Sigma) (Pyr-actin) as previously described (35).

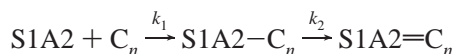
**Cross-Linking Reactions.** For the cross-linking reactions the following buffers were used: 50 mM Tris-HCl, pH 8.0, 0.1 mM ADP, 0.2 mM  $\text{MgCl}_2$ , and 0.1 M KCl (MgADP, pH 8.0); 50 mM imidazole, pH 7.0, 0.1 mM ADP, 0.2 mM

$\text{MgCl}_2$ , and 0.1 M KCl (MgADP, pH 7.0); 50 mM Tris-HCl, pH 8.0, and 0.1 M KCl (rigor, pH 8.0). All cross-linking reactions were carried out on ice ( $4^\circ\text{C}$ ). After incubation of 20  $\mu\text{M}$  S1A2 for 40 min in the appropriate buffer, a 2-fold molar excess of the cross-linker over the protein was added. Solutions of the cross-linkers were freshly prepared by diluting (1:10) the stock solutions ( $\sim 10\text{ mM}$  in methanol) with the appropriate buffer (see above). The exact concentration of the cross-linker solution was determined by adding an excess of  $\beta$ -mercaptoethanol in an aliquot and measuring the absorption of the released 2-nitro-5-thiobenzoate (NTB<sup>−</sup>) at 412 nm, using a molar extinction coefficient  $\epsilon_{412} = 14\,150\text{ M}^{-1}\text{ cm}^{-1}$  (36). The cross-link reaction was followed spectrophotometrically at 412 nm by the release of NTB<sup>−</sup>. Simultaneously, aliquots were taken for measuring the time course of the  $Ca^{2+}$ - and  $K^+$ (EDTA)-ATPase activity during the modification. All experiments were carried out at least twice.

**ATPase Measurements.** All ATPases were measured at  $30^\circ\text{C}$  by a malachite green method (37). For  $Ca^{2+}$ -ATPase measurements a buffer containing 50 mM Tris-HCl, pH 7.5, 0.25 M KCl, 5 mM  $\text{CaCl}_2$ , and 0.2 mM ATP (Boehringer) was used.  $K^+$ (EDTA)-ATPases were measured in a buffer containing 50 mM Tris-HCl, pH 7.5, 1 M KCl, 5 mM EDTA, and 0.2 mM ATP. Standard calibration curves were established for each ATPase buffer using  $\text{KH}_2\text{PO}_4$ . In the ATPase assay the ATP concentration was reduced to 0.2 mM in order to avoid high background values.  $Ca^{2+}$ -ATPase activity with the lowered ATP concentration was checked for linearity by increasing the amount of S1A2. A typical ATPase assay contained 5  $\mu\text{L}$  of 20 mM ATP and 495  $\mu\text{L}$  ATPase buffer containing  $(2\text{--}7) \times 10^{-3}\text{ mg}$  of S1A2. After 1, 2, 3, 4, and 5 min incubation time 500  $\mu\text{L}$  of ice-cold 0.6 M PCA was added and the procedure continued as described (37). Twin values were fitted with the program Grafit (Ericathus software), and  $k_{\text{cat}}$  values ( $\mu\text{mol}$  of  $\text{P}_i\text{ min}^{-1}\text{ mg}^{-1}$ ) were determined from the slope. Typical  $k_{\text{cat}}$  values for different S1 preparations were 0.8–1.2  $\mu\text{mol}$  of  $\text{P}_i\text{ min}^{-1}\text{ mg}^{-1}$  for the  $Ca^{2+}$ -ATPase activity and 1.2–1.6  $\mu\text{mol}$  of  $\text{P}_i\text{ min}^{-1}\text{ mg}^{-1}$  for the  $K^+$ (EDTA)-ATPase activity.

For ATPase measurements during protein modification aliquots of 20  $\mu\text{L}$  were taken at the appropriate time and diluted immediately in 80  $\mu\text{L}$  of ATPase buffer. From this solution 17  $\mu\text{L}$  was directly added to 478  $\mu\text{L}$  of ATPase buffer together with 5  $\mu\text{L}$  of 20 mM ATP. ATPase activity was measured for 1.5 min for both the  $Ca^{2+}$ -ATPase and  $K^+$ (EDTA)-ATPase. All values were taken twice.

**Kinetic Analysis of the  $Ca^{2+}$ -ATPase.** The kinetic analysis of the time course of the  $Ca^{2+}$ -ATPase during protein modification was carried out as described (38). Regarding the thiols of S1A2 to be reacted with the cross-linkers ( $C_n$ ), the following assumptions were made: (a) there are three thiols involved, SH1, SH2, and  $\text{SH}_{\text{LC}}$  (the thiol of the A2 light chain); (b) the modification of SH1 with  $C_n$  is faster than modification of SH2; (c) cross-linking to SH2 occurs before SH2 is modified by a second molecule of  $C_n$ ; (d) the reaction rate of  $\text{SH}_{\text{LC}}$  with  $C_n$  is very slow in comparison to the reaction rate of SH1; i.e.,  $[C_n]$  has not to be corrected for that part reacting with  $\text{SH}_{\text{LC}}$ ; and (e) the reaction of the cross-linker with  $\text{SH}_{\text{LC}}$  does not alter the  $Ca^{2+}$ -ATPase of S1A2,  $\text{S1A2}-C_n$ , or  $\text{S1A2}=\text{C}_n$ . According to these assumptions, the reaction scheme is



where  $\text{C}_n$  is the unreacted cross-linker,  $\text{S1A2-C}_n$  is S1A2 with SH1 reacted with one end of  $\text{C}_n$ ,  $\text{S1A2=C}_n$  is S1A2 cross-linked between SH1 and SH2, and  $k_1$  and  $k_2$  are the rate constants for activation and inactivation of the  $\text{Ca}^{2+}$ -ATPase activity. The rate equations are

$$d[\text{S1A2}]/dt = -k_1[\text{S1A2}][\text{C}_n] \quad (1)$$

$$d[\text{C}_n]/dt = -k_1[\text{S1A2}][\text{C}_n] \quad (2)$$

$$d[\text{S1A2-C}_n]/dt = k_1([\text{S1A2}][\text{C}_n]) - k_2[\text{S1A2-C}_n] \quad (3)$$

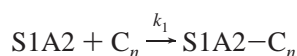
$$d[\text{S1A2=C}_n]/dt = k_2[\text{S1A2-C}_n] \quad (4)$$

The  $\text{Ca}^{2+}$ -ATPase activity ( $V$ ) of S1A2 in the presence of the cross-linkers is given by

$$V = V_0[\text{S1A2}] + V_1[\text{S1A2-C}_n] + V_2[\text{S1A2=C}_n] \quad (5)$$

where  $V_0$ ,  $V_1$ , and  $V_2$  are the  $\text{Ca}^{2+}$ -ATPase activities of unmodified, SH1-modified, and SH1-SH2 cross-linked S1A2, respectively. Since the rate equations cannot be solved analytically, the reaction progress curves were calculated by numeric integration using the program Scientist (Micro Math Scientific Software, Salt Lake City, UT), with variable values for  $k_1$ ,  $k_2$ , and  $V_1$ . For  $V_0$  and  $V_2$  the ATPase activities before modification (100% activity) and after complete modification (5–10% activity) were taken.

**Kinetic Analysis of the  $\text{K}^+(\text{EDTA})$ -ATPase.** The following assumptions were made: (a) modification of SH1 with  $\text{C}_n$  is faster than modification of SH2; (b) cross-linking to SH2 will not alter the  $\text{K}^+(\text{EDTA})$ -ATPase activity; (c) the reaction rate of  $\text{SH}_{\text{LC}}$  with  $\text{C}_n$  is very slow in comparison to the reaction rate of SH1; and (d) the reaction of the cross-linker with  $\text{SH}_{\text{LC}}$  does not alter the  $\text{K}^+(\text{EDTA})$ -ATPase. The kinetic analysis of the time course of the  $\text{K}^+(\text{EDTA})$ -ATPase was carried out according to the scheme



where  $\text{C}_n$  is the unreacted cross-linker,  $\text{S1A2-C}_n$  is S1A2 with SH1 reacted with one end of  $\text{C}_n$ , and  $k_1$  is the rate constant for the inactivation of the  $\text{K}^+(\text{EDTA})$ -ATPase. The rate equations are

$$d[\text{S1A2}]/dt = -k_1[\text{S1A2}][\text{C}_n] \quad (6)$$

$$d[\text{C}_n]/dt = -k_1[\text{S1A2}][\text{C}_n] \quad (7)$$

$$d[\text{S1A2-C}_n]/dt = k_1[\text{S1A2}][\text{C}_n] \quad (8)$$

The  $\text{K}^+(\text{EDTA})$ -ATPase activity ( $V$ ) of S1A2 in the presence of the cross-linkers is given by

$$V = V_0[\text{S1A2}] + V_1[\text{S1A2-C}_n] \quad (9)$$

where  $V_0$  and  $V_1$  are the  $\text{K}^+(\text{EDTA})$ -ATPase activities of unmodified and SH1-modified S1A2, respectively. For  $V_0$  and  $V_1$  the ATPase activities before modification (100% activity) and after complete modification (1–5% activity) were taken. The data were fitted as described above.

**Reactivity of the Cross-Linking Reagents with G-Actin and L-Cysteine.** These experiments were performed in order to check the reactivity of the cross-linking reagents with single thiol groups in a protein and a low molecular weight compound. Titrations were carried out with 10  $\mu\text{M}$  G-actin, or 10  $\mu\text{M}$  L-cysteine (Sigma), in a buffer containing 50 mM imidazole, pH 7.0 (G-actin and L-cysteine), or 10 mM Tris-HCl, pH 8.0 (G-actin), in a 20 °C thermostated water bath using a 10-fold molar excess of the cross-linking reagents  $\text{C}_n$  ( $n = 0, 3, 6, 7, 8, 9, 10$ , and 12). Modification was followed by measuring the absorbance at 412 nm (release of  $\text{NTB}^-$ ). Data were fitted with the program Grafit (Ericathus software) using pseudo-first-order kinetics.

**Synthesis of the Cross-Linking Reagents  $\text{ArSS}-(\text{CH}_2)_n-\text{SSAr}$  ( $\text{C}_n$ ).** Cross-linking reagents with  $n = 3, 6$ , or 9 have been described (39, 40). Cross-linking reagents with  $n = 8$  or 10: To 0.555 mmol of 5,5'-dithiobis(2-nitrobenzoic acid) (Ellman's reagent, Sigma), dissolved in 10 mL of 0.1 M Tris-HCl, pH 7.5, 0.185 mmol of 1,8-octanedithiol (Aldrich), or 1,10-decanedithiol (Lancaster), was added with vigorous stirring. The reaction was kept for 3 h at 25 °C and the pH adjusted to 7–7.5 with 1 M NaOH from time to time. The reaction was stopped by addition of 32% HCl until a pH of 0–1 was reached. The precipitate was isolated by filtration and twice extracted with ether. The ether was partly removed in vacuo, and methanol was added to prevent complete drying. The methanolic solution was submitted to preparative thin-layer chromatography (TLC) using silica plates 20 × 20 cm (60F<sub>254</sub>, Merck) in chloroform/methanol/2 N acetic acid [65/25/4 (v/v/v)]. The band containing the cross-linking reagent was identified in UV light and separated from Ellman's reagent and  $\text{NTB}^-$  both located below, extracted with methanol, and concentrated by evaporation in vacuo to a final concentration of ca. 10 mM. The cross-linker solutions were stored in methanol at 4 °C. Cross-linking reagents with  $n = 7$  or 12: 1,7-heptanedithiol and 1,12-dodecanedithiol were not commercially available. They were prepared as follows (41): 7.62 mmol of 1,12-dibromododecane (Lancaster) or 1,7-dibromoheptane (Aldrich) was heated under reflux with 16.76 mmol of thiourea (Merck) in 5 mL of 95% ethanol for 6 h. The reaction mixture was saponified with 5 mL of 5 M NaOH by heating under reflux and  $\text{N}_2$  gas for 2 h. Then 2 N HCl was added to the cooled reaction mixture. The acidic mixture was extracted with ether, and the ether was evaporated in vacuo, resulting in a solid (25 °C) fatty substance or oily liquid, identified by TLC (see above) as the corresponding alkylenedithiols. Reaction of 1,12-dithiododecane or 1,7-dithioheptane with excess of Ellman's reagent was as described above.

**Position of the Cross-Link.** The position of the cross-link was determined by using either fluorescent or radioactive labeling of the thiol groups. (1) Fluorescent label. The analysis was performed according to Sutoh (42) with the  $\text{S1A2=C}_9$  derivative using DACM (Aldrich). Gel analysis was carried out as described (43, 44). (2) Radioactive label. The modifications were carried out as described (42) with S1A2,  $\text{S1A2=C}_0$ ,  $\text{S1A2=C}_3$ , and  $\text{S1A2=C}_9$  using  $^{14}\text{C}$ -NEM (NEN) as a radioactive label instead of DACM. The radioactively labeled conjugates were digested with trypsin. Analysis was carried out using SDS-PAGE (43, 44). The radioactive gels were stained with Coomassie Brilliant Blue and dried on Whatman paper. Radioactive gel bands were



detected using the Molecular Imaging screen BI, the GS-363 sample loading dock, the GS-363 Molecular Imager System, and the Molecular Analyst software (Bio-Rad).

The purified  $^{14}\text{C}$ -NEM-labeled S1A2=C<sub>9</sub> conjugate (6.2 mg) was lyophilized and digested with BrCN (Serva) as described (45). TFA-soluble and TFA-insoluble BrCN peptides were analyzed by HPLC using a reversed-phase C-18 column with an attached guard cartridge (Knauer, Nucleosil, 100 C-18, 4 mm i.d.  $\times$  25 cm, 5  $\mu\text{m}$  packing material) on a Waters HPLC system (Eschborn, Waters 996 photodiode array detector, Waters 600 pump, Waters 600 controller, Millenium software). Solvent A was 0.6% TFA in H<sub>2</sub>O and solvent B was 0.6% TFA in 60% CH<sub>3</sub>CN. The flow rate was 1 mL/min and the temperature was 25 °C. Gradients: 0–1 min, 100% A; 1–31 min, 0–30% B, linear gradient; 31–36 min, 30–60% B, linear gradient; 36–40 min, 60% B; 40–45 min, 60–0% B, linear gradient. Peptides were detected by their absorbance at 220 nm. Fractions were screened for radioactivity by liquid scintillation counting.

**Actin Affinity—Stopped-Flow Experiments.** The rate of actin binding ( $k_{\text{on}}$ ) and rate constants for actin dissociation from S1A2, S1A2=C<sub>0</sub>, or S1A2=C<sub>10</sub> ( $k_{\text{off}}$ ) were determined as described (46). The dissociation equilibrium constant ( $K_{\text{d}}$ ) for actin binding to different S1A2 derivatives was calculated from the ratios of  $k_{\text{off}}$  and  $k_{\text{on}}$  (35, 47). The stopped-flow experiments for transient kinetics were performed at 20 °C with a Hi-Tech Scientific SF61 stopped-flow spectrophotometer. The observation cell had a 10 mm excitation path and fluorescence and fluorescence emission via 10  $\times$  1.5 mm<sup>2</sup> windows. Pyr-actin fluorescence was excited at 365 nm and detected after passage through a KV 389 nm cutoff filter. Data were stored and analyzed using software provided by Hi-Tech. Transients are the average of three to five consecutive shots of the stopped-flow machine. The experimental buffer used was 20 mM imidazole, pH 7.0, 5 mM MgCl<sub>2</sub>, and 100 mM KCl.

**Regeneration Experiments.** To show that modification of S1A2 with the cross-linkers had not caused denaturation of the protein, the S1A2 conjugates were reduced during 24 h dialysis against 50 mM imidazole, pH 7.0, and 10 mM DTT at 4 °C. The Ca<sup>2+</sup>-ATPases and K<sup>+</sup>(EDTA)-ATPases for the reduced S1A2 were determined. The amount of cross-linker monovalently reacted with S1A2 was determined by addition of 10 mM DTT to the S1A2 conjugates and measurement of the absorbance of the released NTB<sup>−</sup> at 412 nm.

## RESULTS

**Reagents.** The thiol-specific cross-linking reagents used in this study were prepared from  $\alpha,\omega$ -alkylenedithiols and Ellman's reagent. As activated disulfides (Figure 1) the cross-linkers easily reacted with thiols in a disulfide exchange reaction that proceeded exclusively via the route forming the dialkyl disulfide, with release of 1 equiv of NTB<sup>−</sup>. Similarity with the reaction of Ellman's reagent allowed us to include Ellman's reagent as a 2 Å cross-linker in the series. Together with other reagents of the same type prepared and characterized in previous studies (39, 48), we used eight reagents with cross-linking spans from 2.0 to 20.3 Å. It was of considerable value that all reactions with the novel reagents could be monitored for their kinetics and stoichiometry by spectrophotometry, an advantage not offered by

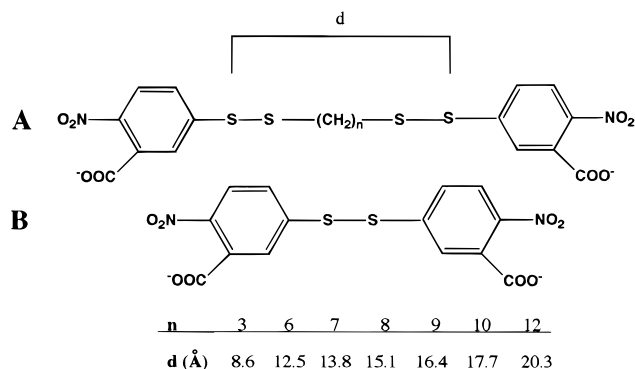


FIGURE 1: Structures and cross-linking spans ( $d$ ) of the cross-linking reagents  $C_n$ . (A) As activated disulfides the cross-linkers  $C_n$  ( $n = 3, 6, 7, 8, 9, 10$ , and  $12$ ) easily react with thiols in a disulfide exchange reaction that exclusively proceeds under formation of the dialkyl disulfide and release of 1 equiv of NTB<sup>−</sup>, which can be monitored at 412 nm. (B) The cross-linking span of Ellman's reagent ( $C_0$ ) was assumed as the distance between the sulfur atoms in a disulfide, i.e., ca. 2 Å.

Table 1: Pseudo-First-Order Rate Constants for the Modification of G-Actin (Cys<sub>374</sub>) and L-Cysteine with the Cross-Linking Reagents  $C_n$ <sup>a</sup>

$C_n$	G-actin, pH 8 $k_A$ ( $10^{-3} \text{ s}^{-1}$ )	G-actin, pH 7 $k_A$ ( $10^{-3} \text{ s}^{-1}$ )	L-cysteine, pH 7 $k'$ ( $10^{-3} \text{ s}^{-1}$ )
$C_0$	$3.4 \pm 0.1$	$4.2 \pm 0.2$	$114 \pm 3$
$C_3$	$9.7 \pm 0.5$	$11.1 \pm 0.4$	$18.8 \pm 0.15$
$C_6$	$9.7 \pm 0.3$	$8.1 \pm 0.1$	$9.1 \pm 0.1$
$C_7$	$10.5 \pm 0.2$	$8.8 \pm 0.2$	$9.4 \pm 0.1$
$C_8$	$16.4 \pm 0.2$	$16 \pm 0.6$	$9.3 \pm 0.1$
$C_9$	$30 \pm 0.6$	$21.5 \pm 1.5$	$10.2 \pm 0.1$
$C_{10}$	$33.8 \pm 0.8$	$22.3 \pm 1$	$8.9 \pm 0.25$
$C_{12}$			$7.18 \pm 0.3$

<sup>a</sup> The modifications were carried out with 10  $\mu\text{M}$  G-actin or 10  $\mu\text{M}$  L-cysteine at 20 °C in 10 mM Tris-HCl, pH 8.0 (G-actin or L-cysteine), or 50 mM imidazole, pH 7.0 (G-actin), with an excess of 10 equiv of the reagents  $C_n$  and were followed spectrophotometrically at 412 nm (release of NTB<sup>−</sup>). All titrations were fitted by pseudo-first order kinetics. It was not possible to determine the rate constant for the modification of G-actin with  $C_{12}$  because of partial unfolding of G-actin in the presence of this reagent.

most previous thiol reagents. Moreover, linkage of the reagent to the protein was in all cases by a cystine-type disulfide that could easily be cleaved with, e.g., DTT, thus allowing controls for possible loss of biological activity due to denaturation of the protein.

All reagents (except those with  $n = 0$  and 3) reacted with low molecular weight thiols (e.g., cysteine) at a similar rate ( $k'$  ca.  $1 \times 10^{-2} \text{ s}^{-1}$ ; Table 1) but showed an increase in the reaction rate with increasing length of their hydrocarbon chains when reacted with protein thiols. A similar increase in rate was found for the reaction of SH1 in the myosin head (Table 2). Since the effect was seen with protein thiols only and not with cysteine, it may be explained by an interaction of the growing hydrophobic mass of the reagents with hydrophobic domains of the proteins. As a consequence of this effect all kinetic values derived from reactions of S1A2 with the reagents had to be corrected for this intrinsic property of the reagents (see below and Table 2).

**Thiol Modification of S1A2 in the Presence of MgADP.** The reactions of S1A2 with 2 equiv of  $C_n$  ( $n = 0, 3, 6, 7, 8, 9, 10$ , and  $12$ ) led to the release of  $3 \pm 0.2$  equiv of NTB<sup>−</sup> in all cases (Figure 2, closed circles), indicating that a cross-

Table 2: Rate Constants  $k_1$  and Normalized Rate Constants ( $k_1/k_A$ ) for the Modification of SH1 with the Cross-Linking Reagents  $C_n$ <sup>a</sup>

$C_n$	MgADP, pH 8.0 (1)		MgADP, pH 7.0 (2)		rigor, pH 8.0 (3)	
	$k_1$ ( $\mu\text{M}^{-1} \times 10^{-4} \text{ s}^{-1}$ )	$k_1/k_A$	$k_1$ ( $\mu\text{M}^{-1} \times 10^{-4} \text{ s}^{-1}$ )	$k_1/k_A$	$k_1$ ( $\mu\text{M}^{-1} \times 10^{-4} \text{ s}^{-1}$ )	$k_1/k_A$
$C_0$	$1.17 \pm 0.2$	0.34	$0.53 \pm 0.1$	0.16	$0.11 \pm 0.03$	0.032
$C_3$	$2.83 \pm 0.6$	0.29	$1.23 \pm 0.3$	0.13	$0.88 \pm 0.32$	0.091
$C_6$	$3.67 \pm 0.8$	0.38	$2.65 \pm 0.4$	0.27	$1.79 \pm 0.45$	0.18
$C_7$	$4.53 \pm 0.9$	0.43	$2.42 \pm 0.2$	0.23	$4.07 \pm 0.39$	0.42
$C_8$			$3.07 \pm 0.7$	0.19	$7.0 \pm 0.87$	0.42

<sup>a</sup> The reactions were carried out on ice in 50 mM Tris-HCl, pH 8.0, 0.1 mM ADP, 0.2 mM  $\text{MgCl}_2$ , and 0.1 M KCl (1), in 50 mM imidazole, pH 7.0, 0.1 mM ADP, 0.2 mM  $\text{MgCl}_2$ , and 0.1 M KCl (2), or in 50 mM Tris-HCl, pH 8.0, and 0.1 M KCl (3). Rate constants  $k_1$  were fitted using the time course of the  $\text{K}^+(\text{EDTA})$ -ATPase activity. Normalization of  $k_1$  was performed using  $k_{A(\text{pH } 8)}$  (Table 1).

link must have been formed. The fourth reactive group was covalently bound to the protein, as seen from the UV absorption spectrum of the S1A2 conjugate after gel filtration, exhibiting a shoulder at 340 nm (not shown). For the exact determination of the amount of monovalently bound cross-linker per mole of S1A2, the amount of  $\text{NTB}^-$  released after treatment with DTT was measured at 412 nm and found to be ca. 1:1 in all conjugates. The sum of released and attached (unreacted) thiol-capturing moieties thus totaled ca. 4 in all cases.

**Spectrophotometry.** Kinetics of the modification of the three thiols in S1A2 were followed spectrophotometrically at 412 nm for all reagents (Figure 2, closed circles). Rates of modification increased strongly with increasing length of the hydrocarbon chains of the reagents, reached a maximum for the reaction with  $C_8$  and  $C_9$ , and decreased for  $C_{10}$  and further for  $C_{12}$  ( $C_0 < C_3 < C_6 < C_7 < C_8 \approx C_9 > C_{10} > C_{12}$ ). Although the contributions to the overall reaction made by the three types of reactive thiols (SH1, SH2 in the cross-linking reaction, and  $\text{SH}_{\text{LC}}$ ) could not be clearly distinguished, we consider that the first phase of the overall reaction (0.5–1.5 equiv of SH reacted within the first few minutes) was dominated by SH1, while modification of SH2, i.e., the cross-linking reaction, seemed to be the rate-determining step at least for all reagents between  $n = 0$  and 8. This is in line with studies of Wells and Yount (22), and Huston et al. (23), who showed that reaction of S1 with 2 equiv of Ellman's reagent performed under the same conditions as ours proceeded in two steps: a rapid reaction that could be attributed to modification of SH1 and  $\text{SH}_{\text{LC}}$ , as identified by the associated decrease of  $\text{K}^+(\text{EDTA})$ - and increase in  $\text{Ca}^{2+}$ -ATPase activities (modification of  $\text{SH}_{\text{LC}}$  was assumed to have no influence on the ATPase activities), and a slower step, attributable to the cross-linking reaction between SH1 and the neighboring SH2 as identified by the associated decrease in  $\text{Ca}^{2+}$ -ATPase activity. These correlations were found to hold for other kinds of reagents as well (14–16) and, as shown in the present study, are valid also for our series of cross-linking reagents except for  $C_{10}$  and  $C_{12}$ , which may decrease  $\text{Ca}^{2+}$ -ATPase activity already after reaction of SH1 (unpublished results).

**$\text{K}^+(\text{EDTA})$ -ATPase.** Modification of SH1 as reflected by the rate of  $\text{K}^+(\text{EDTA})$ -ATPase decrease was determined at pH 8 for the reagents  $C_0$ ,  $C_3$ ,  $C_6$ , and  $C_7$  (Figure 3). Reaction rates ( $k_1$ ) increased with increasing chain length of the cross-linking reagents, as shown in Table 2. Correction of the  $k_1$

Table 3: Cross-Linking Rates  $k_2$  and Normalized Cross-Linking Rates ( $k_2/k_1$ ) for the Reaction of S1A2 with 2 equiv of the Cross-Linking Reagents  $C_n$ <sup>a</sup>

$C_n$ (cross-linking span)	MgADP, pH 8.0 (1)		MgADP, pH 7.0 (2)		rigor, pH 8.0 (3)	
	$k_2$ ( $10^{-4} \text{ s}^{-1}$ )	$k_2/k_1$	$k_2$ ( $10^{-4} \text{ s}^{-1}$ )	$k_2/k_1$	$k_2$ ( $10^{-4} \text{ s}^{-1}$ )	$k_2/k_1$
$C_0$ (2.0 Å)	$3.3 \pm 0.6$	6.22	$0.73 \pm 0.1$	1.38		
$C_3$ (8.6 Å)	$8.3 \pm 0.8$	6.8	$1.2 \pm 0.1$	1.03	$0.6 \pm 0.2$	0.49
$C_6$ (12.5 Å)	$16.2 \pm 3.3$	6.11	$2.0 \pm 0.3$	0.8	$1.0 \pm 0.2$	0.38
$C_7$ (13.8 Å)	$28.2 \pm 6.2$	11.6	$5.3 \pm 0.6$	2.19	$1.8 \pm 0.2$	0.74
$C_8$ (15.1 Å)			$10.5 \pm 2.3$	3.42	$2.7 \pm 0.5$	0.88

<sup>a</sup> Experimental conditions as in Table 2. The cross-linking rate  $k_2$  was fitted using the time course of the  $\text{Ca}^{2+}$ -ATPase activity for those reactions where an activation and deactivation phase was observed. The normalized cross-linking rates  $k_2/k_1$  were calculated by using  $k_{1(\text{MgADP, pH } 7)}$  as standard (see Table 2).

values for the intrinsic properties of the reagents as achieved by relating  $k_1$  to the rate constants of actin titration ( $k_1/k_A$ ; see Table 2) yielded constant values, indicating that the increase observed was solely due to the acceleration caused by the increasing length of the reagents. In the corresponding experiments at pH 7 a similar effect was observed although all reaction rates were somewhat reduced, probably due to a lower degree of deprotonization of SH1 at pH 7. We conclude from these data that the relative reactivity of SH1 is not significantly changed by the pH shift. In contrast, there was a distinct change in reactivity of SH1 in the absence of the nucleotide (see below).

**$\text{Ca}^{2+}$ -ATPase.** The rate of the  $\text{Ca}^{2+}$ -ATPase decrease (Figure 2, open circles), attributable to the cross-linking reaction, showed that also these rates increased with increasing length of the reagents, but with a steeper gradient than the rates of SH1 modification. According to Polosukhina and Highsmith (38), calculation of  $k_2$  values was possible only for reactions showing an activation and deactivation phase of the  $\text{Ca}^{2+}$ -ATPase, i.e., for the reagents  $C_0$ ,  $C_3$ ,  $C_6$ , and  $C_7$  (Table 3). To eliminate the hydrophobicity effect, also  $k_2$  values were corrected by dividing them for example by  $k_{1(\text{MgADP, pH } 7)}$ . (A corresponding correction could have been made using  $k_A$ , or  $k_{1(\text{MgADP, pH } 8)}$ , yielding similar results; not shown.) From the normalized values  $k_2/k_1$  (Table 3, Figure 5) it was clear that the cross-linking rates were fairly constant for  $C_0$ ,  $C_3$ , and  $C_6$  but increased steeply for  $C_7$ . Anticipating that the distance between SH1 and SH2 would be indicated by the cross-linking span of that reagent that had the highest cross-linking rate (i.e., the highest  $k_2/k_1$  value), namely,  $n \geq 7$ , we derived a distance of  $\geq 14$  Å. A more precise determination was not possible at pH 8, since the activation phase disappeared for higher members but could be performed at pH 7. Probably due to the retarded disulfide exchange reaction at the lower pH, the reagent  $C_8$  also developed an activation phase (Figure 4, Table 2), and processing of the kinetic data (Table 3) demonstrated a further increase in the reaction rate between  $n = 7$  and  $n = 8$  (Figure 5). Assuming that the conformation was not changed significantly by the pH shift, the distance value between SH1 and SH2 in the presence of MgADP can thus be corrected to a value of  $\geq 15$  Å. It is worth noting that the experiments at pH 7 can be regarded as a second, independent determination of the distance value, because at the lower pH all reactions proceeded at ca. 5 times lower rate (Figure 5).

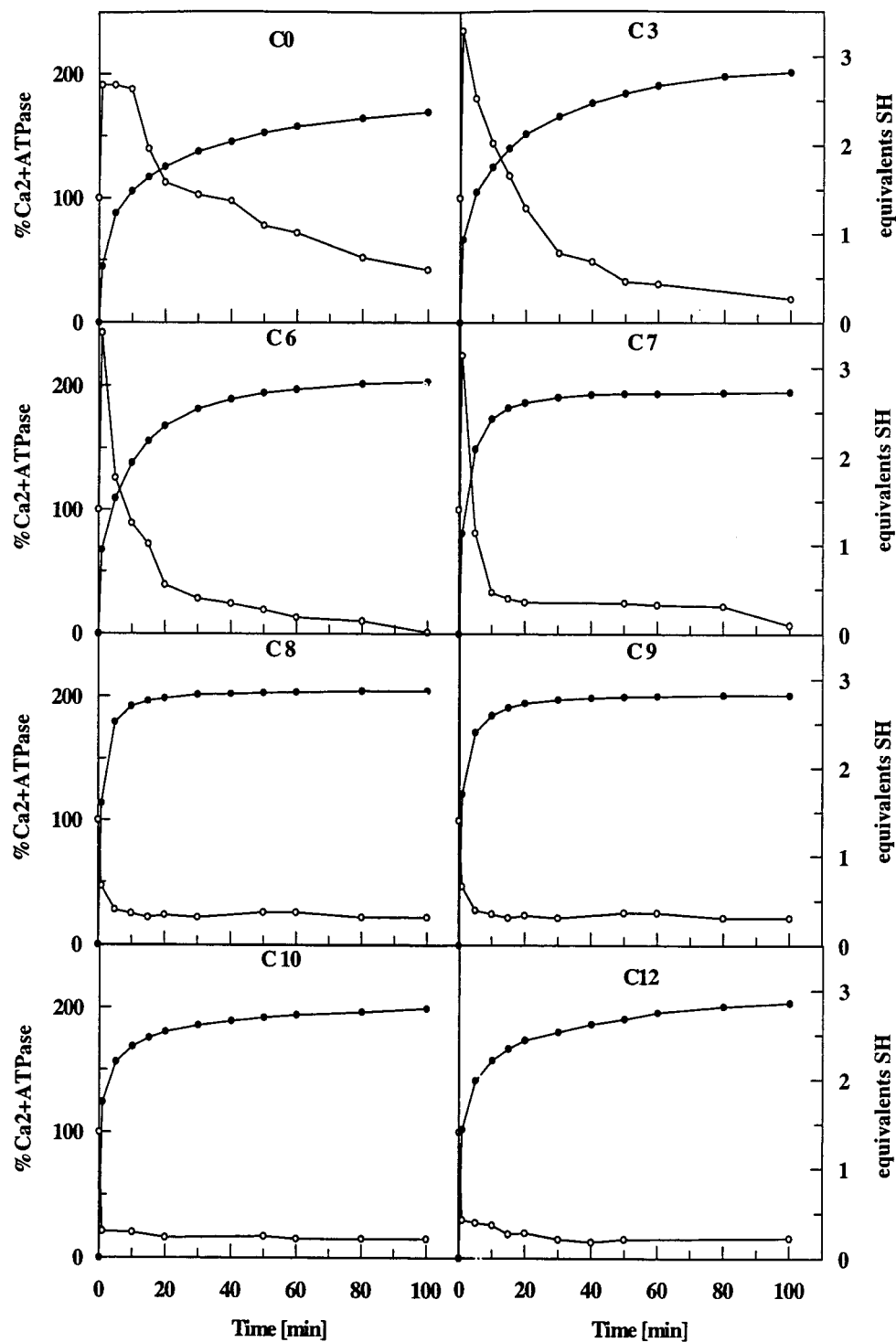


FIGURE 2: Relative  $\text{Ca}^{2+}$ -ATPase activity in the presence of MgADP at pH 8.0 and equivalents of SH groups reacted plotted versus time of modification of S1A2 with the cross-linking reagents  $\text{C}_n$ . S1A2, (20  $\mu\text{M}$ ) was reacted at 4  $^\circ\text{C}$  with 40  $\mu\text{M}$   $\text{C}_n$  ( $n = 0, 3, 6, 7, 8, 9, 10$ , and 12) in 50 mM Tris-HCl, pH 8.0, 0.1 mM ADP, 0.2 mM  $\text{MgCl}_2$ , and 0.1 M KCl. Modification was followed at 412 nm by the release of  $\text{NTB}^-$  and was plotted as equivalents of SH groups modified per mole of S1A2 ( $\lambda$ ). Simultaneously, aliquots were taken for the measurement of the  $\text{Ca}^{2+}$ -ATPase activity ( $\circ$ ). The 100% values of the  $\text{Ca}^{2+}$ -ATPase activity corresponded to 10.5–13.5 nmol of  $\text{P}_i$  hydrolyzed per  $7.82 \times 10^{-3}$  mg of S1A2 in 1.5 min in 500  $\mu\text{L}$  of  $\text{Ca}^{2+}$ -ATPase buffer.

#### Thiol Modification of S1A2 in the Absence of Nucleotide.

In the absence of nucleotide, the reaction also proceeded to 3 equiv of SH, but at a much lower rate (Figure 6A, vs Figure 2). Here, too, cross-links were formed between SH1 and SH2, in addition to monovalent substitution of  $\text{SH}_{\text{LC}}$ . Absence of the nucleotide affected the kinetics of both SH1 modification ( $k_1$ ) and the cross-linking reaction ( $k_2$ ). For  $k_1$ , the correlation with chain length of the reagents was entirely different from

that seen for the nucleotide complex: While the short and hydrophilic reagent  $\text{C}_0$  reacted very slowly, the higher members reacted at strongly accelerated rates, resulting, for example, in similar  $k_1$  values for the reagent  $\text{C}_7$  in the presence and absence of MgADP. While for the MgADP complex the increase in rates ( $k_1$ ) between the reagents  $\text{C}_0$  and  $\text{C}_7$  was ca. 4-fold, it was ca. 40-fold under rigor conditions (Table 2). Such an increase is no longer explain-

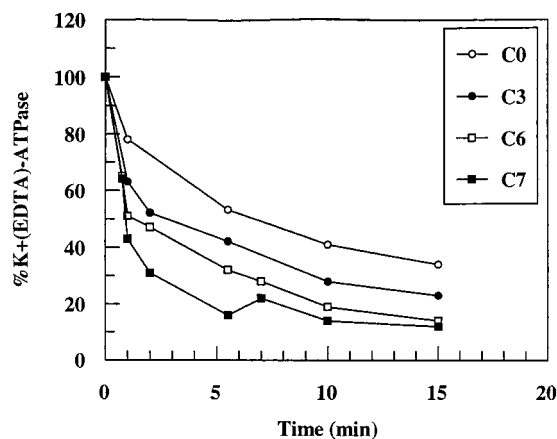


FIGURE 3: Relative K<sup>+</sup>(EDTA)-ATPase activity in the presence of MgADP at pH 8.0 plotted versus time of modification of S1A2 with the cross-linking reagents C<sub>n</sub> (*n* = 0, 3, 6, and 7). Experimental conditions of protein modification were as described in Figure 2. The 100% values of the K<sup>+</sup>(EDTA)-ATPase activity corresponded to 16–18.5 nmol of P<sub>i</sub> hydrolyzed per 7.82 × 10<sup>-3</sup> mg of S1A2 in 1.5 min in 500 μL of K<sup>+</sup>(EDTA)-ATPase buffer. The K<sup>+</sup>(EDTA)-ATPase activities were determined only for the cross-linking reagents which showed an activation phase in the Ca<sup>2+</sup>-ATPase activity (see Figure 2, open circles). The inhibition rate of the K<sup>+</sup>(EDTA)-ATPase activity increased with increasing length of C<sub>n</sub> (see also Table 2).

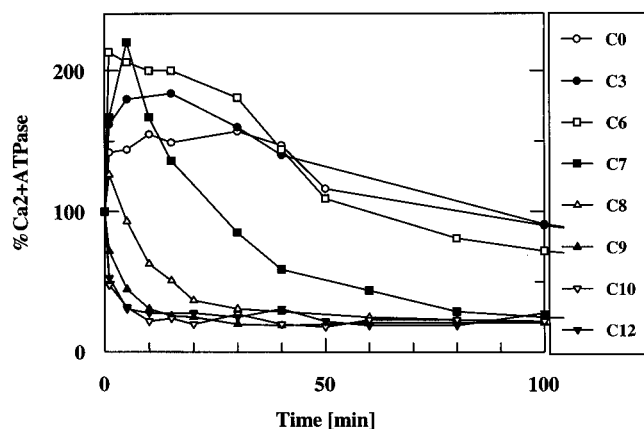


FIGURE 4: Relative Ca<sup>2+</sup>-ATPase activity in the presence of MgADP at pH 7.0 plotted versus time of modification of S1A2 with the cross-linking reagents C<sub>n</sub>. S1A2 (20 μM) was reacted at 4 °C with 40 μM C<sub>n</sub> (*n* = 0, 3, 6, 7, 8, 9, 10, and 12) in a buffer containing 50 mM imidazole, pH 7.0, 0.1 mM ADP, 0.2 mM MgCl<sub>2</sub>, and 0.1 M KCl.

able by the normal hydrophobicity effect and suggests a second effect that increases the steepness of the dependence of SH1 reactivity on hydrocarbon chain length.

Cross-linking rates  $k_2$  in the absence of nucleotide were ca. 15 times lower than in the presence of MgADP (Table 3). As an example, panels A and B of Figure 7 show the fitted data for the reaction of 2 equiv of C<sub>3</sub> with S1A2 at pH 8, in the presence and absence of MgADP, respectively. With increasing length of the reagents, cross-linking rates increased also under rigor conditions. Again, a kinetic analysis was possible only for the shorter reagents C<sub>3</sub>, C<sub>6</sub>, C<sub>7</sub>, and C<sub>8</sub>. The hydrophobicity effect was corrected for by normalization of their  $k_2$  values with  $k_{1(\text{MgADP}, \text{pH} 7)}$ . (Normalization with  $k_A$ , or  $k_{1(\text{MgADP}, \text{pH} 8)}$ , as standard was also performed and gave similar results (not shown); it was not possible with  $k_{1(\text{rigor})}$ , because the ratio of  $k_{1(\text{rigor})}$  to  $k_A$  (Table

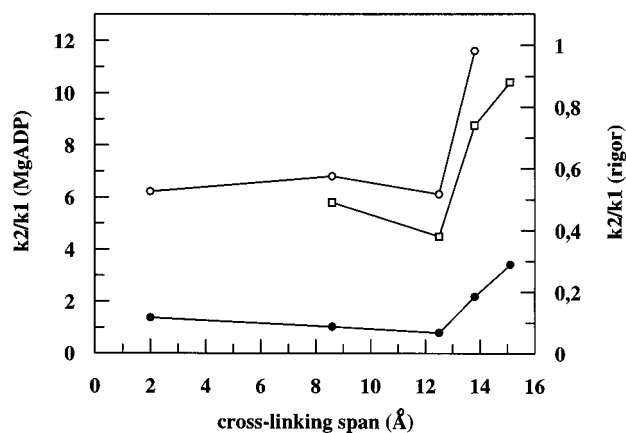


FIGURE 5: Plot of the normalized cross-linking rates  $k_2/k_1$  versus the cross-linking span (Å) of the reagents C<sub>n</sub> (*n* = 0, 3, 6, 7, and 8) as used for modifications of S1A2 in the presence of MgADP at pH 8.0 (○) or pH 7.0 (●) (left scale) or in the absence of MgADP at pH 8 (□) (right scale). The normalized  $k_2/k_1$  values were taken from Table 3.

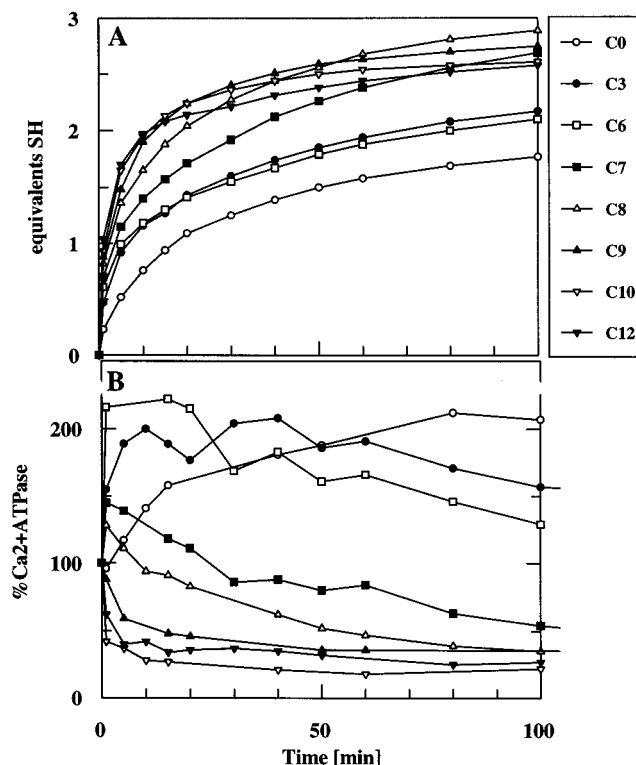


FIGURE 6: Equivalents of SH groups reacted (A) and relative Ca<sup>2+</sup>-ATPase activity (B) in the absence of MgADP at pH 8.0 plotted versus time of modification of S1A2 with the cross-linking reagents C<sub>n</sub>. S1A2 (20 μM) was reacted at 4 °C with 40 μM C<sub>n</sub> (*n* = 0, 3, 6, 7, 8, 9, 10, and 12) in 50 mM Tris-HCl, pH 8.0, and 0.1 M KCl. (A) Modification was followed by the release of NTB<sup>-</sup> at 412 nm and was plotted as equivalents of SH groups modified per S1A2. (B) Simultaneously, aliquots were taken for the measurement of the Ca<sup>2+</sup>-ATPase activity. The 100% values of the Ca<sup>2+</sup>-ATPase activity corresponded to 10.5–13.5 nmol of P<sub>i</sub> hydrolyzed per 7.82 × 10<sup>-3</sup> mg of S1A2 in 1.5 min in 500 μL of Ca<sup>2+</sup>-ATPase buffer.

2), to  $k_{1(\text{MgADP}, \text{pH} 7)}$ , or to  $k_{1(\text{MgADP}, \text{pH} 8)}$ , was not constant, as required for their use as a standard.)

The normalized values of  $k_2$  (Table 3) were plotted in Figure 5 vs the cross-linking span of the reagents and showed, though at a much lower reaction level, a dependence on chain length similar to that seen in the presence of



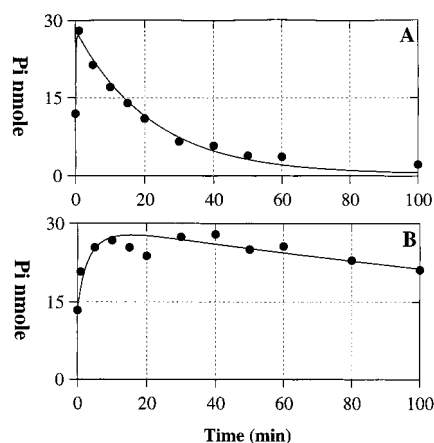


FIGURE 7: Measured (circles) and fitted (line) kinetics of the reaction of 2 equiv of  $C_3$  with S1A2 in the presence of MgADP at pH 8 (A) and in the absence of MgADP at pH 8 (B), expressed as nanomoles of  $P_i$  hydrolyzed per  $7.82 \times 10^{-3}$  mg of S1A2 per 1.5 min in 500  $\mu$ L of  $Ca^{2+}$ -ATPase buffer. The  $P_i$  values at  $t = 0$  min (11.9 and 13.4 nmol of  $P_i$ ), corresponded to the  $k_{cat}$  values of 1.01 (A) and 1.14 (B)  $\mu$ mol of  $P_i$   $min^{-1}$   $mg^{-1}$ . The plot is based on data shown in Figures 2 and 6B.

MgADP. From the similarity of these plots we conclude that there was no change in the distance between SH1 and SH2 when MgADP was removed, i.e., that the distance between the reactive thiols amounted to  $\geq 15$  Å in the absence and presence of the nucleotide.

**Position of the Cross-Link.** The absence of a cross-link between the heavy chain and the light chain was concluded from the absence of a corresponding band of molecular weight 111K in SDS-PAGE (gel not shown). To identify the two thiols involved in the cross-linking reaction, we blocked in one of the cross-linked conjugates, S1A2= $C_9$ , all unreacted thiols with NEM, reduced the product with DTT, and reacted the reduced thiols with DACM, according to Sutoh (42). Digestion of the DACM-labeled conjugate with trypsin caused cleavage of the heavy chain into the 75K

and the 20K fragments as described (49, 50), of which only the 20K fragment containing SH1 and SH2 was fluorescent (gel not shown). The 20K fragment was isolated from the gel and cleaved with hydroxylamine. After cleavage, a faint fluorescence was detected in both the 12K (SH1) and the 5–7K (SH2) fragments (gel not shown), as reported in ref 42.

Since identification of the 5K and 12K fragments by Sutoh's method was unsatisfying, we prepared samples of S1A2 cross-linked with the reagents  $C_0$ ,  $C_3$ , and  $C_9$ , blocked all unreacted thiols with NEM, reduced the product with DTT, and labeled the reduced thiols with  $^{14}C$ -NEM. Radioactivity was found in both the light chain and the heavy chain. Digestion of the conjugates with trypsin revealed similar patterns (70K, 50K, 25K, 20K) for all three conjugates (gel not shown) with the major part of radioactivity in the 20K fragment in all cases. Since Huston et al. (23) had shown that with Ellman's reagent ( $C_0$ ) the cross-link was located between SH1 and SH2, we concluded from the similarity of the gel patterns that in the  $C_3$  and  $C_9$  derivatives of S1 also the cross-links were located between SH1 and SH2. In all cases SH<sub>LC</sub> was not involved in the cross-links but reacted monovalently with 1 equiv of the reagents.

These results were confirmed by another experiment, in which fragmentation of the reduced and labeled material was achieved by BrCN, instead of trypsin. The TFA-soluble part consisted mainly of fragments of the light chain, as concluded from the partial Edman degradation of the corresponding RP18 HPLC-purified peptides. In the TFA-insoluble part, dissolved in NaOH and submitted to RP18 HPLC, the major part of radioactivity was found in one fragment which on rechromatography by HPLC yielded a peptide that by sequencing and mass analysis was identified as the fragment containing SH1 and SH2 (see Figure 8).

**Actin Binding of the S1A2= $C_n$  Derivatives.** Two representative derivatives of the cross-linked S1A2 species, S1A2= $C_0$  and S1A2= $C_{10}$ , were assayed for their affinity for

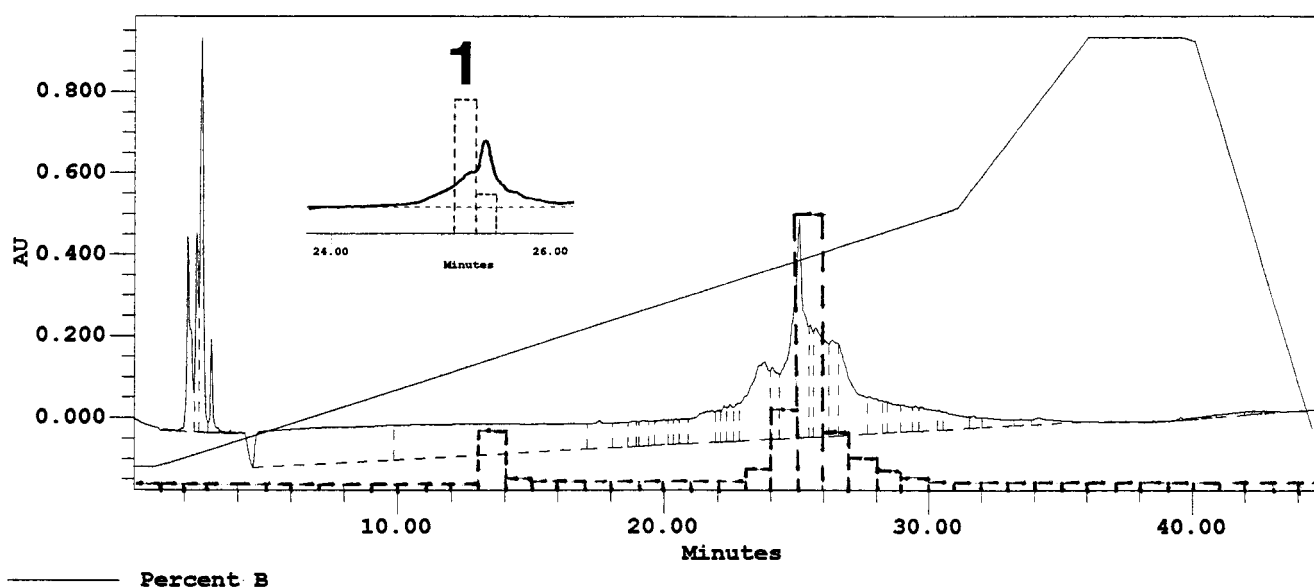


FIGURE 8: Reversed-phase HPLC (RP C-18 column) of the NaOH-soluble BrCN peptides from the  $^{14}C$ -NEM-S1A2= $C_9$  derivative prepared as described under Materials and Methods. Fractions (1 mL) were collected and an aliquot of 20  $\mu$ L was analyzed for radioactivity by liquid scintillation counting. The relative radioactivity profile is shown by the dashed lines. The main radioactive fraction was pooled and rechromatographed under the same conditions (inset). Peak 1, containing 70% of the remaining radioactivity, had the sequence X (E), H, X (E), L, V, L, H, corresponding to the beginning of the BrCN peptide containing SH2 and SH1.



Table 4: Transient Kinetic Analysis of the Actin Binding of S1A2, S1A2=C<sub>0</sub>, and S1A2=C<sub>10</sub><sup>a</sup>

S1A2 derivative	$k_{\text{on}}$ (M <sup>-1</sup> s <sup>-1</sup> )	$k_{\text{off}}$ (s <sup>-1</sup> )	$K_d = k_{\text{off}}/k_{\text{on}}$ (μM)
S1A2	$1.93 \times 10^6$	$0.1 \pm 0.02$	0.052 (0.032*)
S1A2=C <sub>0</sub>	$0.006 \times 10^6$	$0.05 \pm 0.01$	8.3
S1A2=C <sub>10</sub>	$0.008 \times 10^6$	$0.06 \pm 0.01$	7.5
(S1=pPDM*)			(22*)

<sup>a</sup> The stopped-flow experiments were carried out at 20 °C in a buffer containing 20 mM imidazole, pH 7.0, 5 mM MgCl<sub>2</sub>, and 100 mM KCl. For comparison, the  $K_d$  values of S1 and S1 cross-linked with pPDM (S1=pPDM) as determined by Xie and Schoenberg (51) are shown (\*).

F-actin. By stopped-flow measurements,  $k_{\text{on}}$  and  $k_{\text{off}}$  values were determined and  $K_d$  values calculated (Table 4). The affinities of the two derivatives to actin were very similar to each other and much lower (ca. 150×) than that of native S1A2. An actin affinity reduced to a similar extent was reported for S1 cross-linked between SH1 and SH2 with pPDM (51). Such similarity confirms that the cross-links were located between SH1 and SH2.

**Regeneration Experiments.** Reaction of the cross-linkers with S1A2 was fully reversible and caused no denaturation of the protein. On reduction with DTT all S1A2 conjugates restored the K<sup>+</sup>(EDTA)- and the Ca<sup>2+</sup>-ATPase activities to 80–120. [The 100% values were 0.88–1.2 μmol of P<sub>i</sub> min<sup>-1</sup> mg<sup>-1</sup> for the Ca<sup>2+</sup>-ATPase activity, and 1.2–1.6 μmol of P<sub>i</sub> min<sup>-1</sup> mg<sup>-1</sup> for the K<sup>+</sup>(EDTA)-ATPase activity.]

## DISCUSSION

**Microenvironment of SH1.** All thiol modifications in this study are understood as disulfide exchange reactions driven by the release of the mesomeric and stable NTB<sup>-</sup> anion. Since the driving force is the same for all reagents (C<sub>n</sub>), one would expect the reaction kinetics to be similar for all reagents. This is indeed true for the reaction with cysteine (with the exception of C<sub>0</sub> and C<sub>3</sub>) but not for thiols exposed by proteins, such as Cys<sub>374</sub> in G-actin. Here, we found that reaction rates increased with increasing length of the hydrocarbon chain. The effect is probably due to an interaction of the hydrophobic hydrocarbon chains of the reagents with hydrophobic domains in actin resulting in enhanced reaction rates. Such hydrophobicity effect was also seen for the fast-reacting thiol in myosin S1 (Cys<sub>707</sub>, SH1). Acceleration rates with SH1 were similar to those found for Cys<sub>374</sub> of actin as shown by the terms  $k_{1(\text{pH}8, \text{MgADP})/k_A}$  and  $(k_{1(\text{pH}7, \text{MgADP})/k_A})$  in Table 2, which were almost constant. This indicates similar reactivities, and probably microenvironments, for Cys<sub>374</sub> in actin and Cys<sub>707</sub> in myosin S1. Similarity was found only, however, when myosin S1 was in the MgADP complex. Constant values were not obtained with  $k_1$  values of S1 in the absence of nucleotide (see below).

Reactivity of SH1 is known to depend on the nucleotide bound at the active site and was reported to be greater in the presence of MgADP than in its absence (17, 38, 52). The reason for this is probably that nucleotide-induced changes in the active site induce structural changes also in the microenvironment of SH1. In the present study we confirmed the previously reported low reactivity of SH1 in the absence of MgADP, but only for short reagents such as

C<sub>0</sub> and C<sub>3</sub>. It was not found for those of our reagents which possessed longer hydrocarbon chains. Already for C<sub>7</sub> reaction rates of SH1 became similar in the presence and absence of nucleotide. This is a consequence of the fact that in the absence of nucleotide the increase in reaction rates  $k_1$  with chain length was much more pronounced than in the nucleotide-bound state and was obviously not caused by the above hydrophobicity effect alone. Accordingly, the terms  $(k_{1(\text{rigor}, \text{pH}8)/k_A})$  were not constant but increased by a factor of 10 between chain lengths of  $n = 0$  and  $n = 8$  (Table 2). A similar factor of 10 was found for the corresponding ratios  $k_{1(\text{rigor}, \text{pH}8)/k_{1(\text{MgADP}, \text{pH}8)}}$  or  $k_{1(\text{rigor}, \text{pH}8)/k_{1(\text{MgADP}, \text{pH}7)}}$ , suggesting that the effect was significant. We argue that the normal hydrophobicity effect is superposed by a second effect that likewise depends on the hydrophobic nature of the reagents but causes a much sharper increase in reaction rates with increasing length of the hydrocarbon chain. A reasonable explanation for this is that SH1 in the absence of MgADP is shielded by a hydrophobic domain, which can be expected to provide better protection against hydrophilic reagents such as C<sub>0</sub> and C<sub>3</sub> than against more hydrophobic reagents such as C<sub>7</sub>, which might be able to penetrate the domain. Such an explanation would be in line with work of Xing and Cheung (53), who postulated from energy-transfer experiments that SH1 in the absence of nucleotide is in a more hydrophobic environment than in the MgADP complex.

Anticipating that S1 in the absence of nucleotide corresponds to the structure of chicken S1 (1) and that the MgADP complex is closely related to the structure of the *Dictyostelium* S1–MgADP complex (2), such a shielding effect might be provided by loop 501–518 containing Trp<sub>510</sub> and several other hydrophobic residues. In X-ray studies of the MgADP complex this loop could not be localized, probably due to its high flexibility, but in the absence of nucleotide was identified to be close to the SH1/SH2 helix (Figure 9). While in the MgADP complex the flexible loop would allow SH1 to be approached by any kind of reagent, it might cause a steric hindrance in the absence of nucleotide, except for those reagents which are hydrophobic enough to interact with the shielding loop. An even stronger shielding effect of SH1 by this loop than in the absence of nucleotide can be expected to exist in the S1–MgADP·VO<sub>4</sub> complex, as concluded from the X-ray structures (3, 6) and from most recent work by Hiratsuka et al. (54), who showed that in the presence of MgADP·VO<sub>4</sub> SH1 cannot be modified with 5-[(iodoacetamido)ethyl]amino]naphthalene-1-sulfonic acid (I-AEDANS).

**Distance Measurement between SH1 and SH2.** One aim of our study was to determine the distance between the two reactive thiols SH1 and SH2 in the presence and absence of MgADP. In the past, such distances were determined by examining whether a reagent of given dimensions was able to bridge SH1 and SH2 or not. Among the reagents assayed were *p*-phenylenedimaleimide (pPDM, 12–14 Å), which forms a cross-link between SH1 and SH2 in the presence and absence of nucleotide (18), while 4,4'-difluoro-3,3'-dinitrophenyl sulfone (F<sub>2</sub>DPS, 7–10 Å) yielded a cross-link only in the presence of MgADP (21). Even shorter cross-linking reagents such as cobalt phenanthroline (3–5 Å) (19) or Ellman's reagent (22) were able to bridge the two reactive thiols in the S1–MgADP complex, indicating that SH1 and SH2 can come as close as 2 Å and form a disulfide bond.

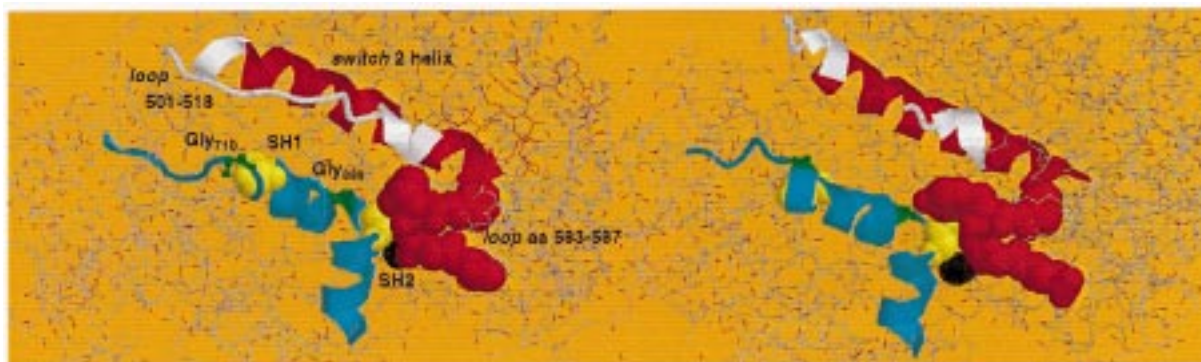


FIGURE 9: View at the SH1/SH2 region of myosin S1 X-ray structures in the absence (left) and presence (right) of MgADP. Left: chicken S1 [PDB file 2MYS (1)]. Right: *Dictyostelium* S1 [PDB file 1MMA (2)]. Shown are the switch 2 helix (red), with its associated loop (white); the broken SH1/SH2 helix (cyan); Cys<sub>707</sub> (Thr<sub>688</sub> in *Dictyostelium* S1) and Cys<sub>697</sub> (Cys<sub>678</sub> in *Dictyostelium* S1) (yellow); the sulfur atom of SH2 (black); Gly<sub>699</sub> and Gly<sub>710</sub> (Gly<sub>680</sub> and Gly<sub>691</sub> in *Dictyostelium* S1) (green); and loop 583–587 (red). For details see text.

In the present study all reagents of the novel type, ranging in length from 2 to 20.3 Å, were able to span the distance between the two thiols. This finding is in agreement with previous results but raises the question of whether the distance between two reactants can be measured simply from the occurrence of the cross-linking event. As already suggested by Reisler and co-workers (26, 27), such an analysis should include kinetic data on the cross-linking reactions, which indeed varied widely for the various reagents used so far. We performed such a kinetic study using our set of reagents and tried to identify which of the reagents would show an optimal fit to the distance between the two thiols as indicated by the fastest cross-linking kinetics. As outlined above, the measured cross-linking rates  $k_2$  had to be corrected for the hydrophobicity effect, for example, by dividing them through  $k_1(\text{MgADPpH7})$  values.

Reaction rates  $k_1$  were derived from the time course of  $\text{K}^+(\text{EDTA})$ -ATPase activity, while the rates of the cross-linking reaction,  $k_2$ , were calculated from the kinetics of  $\text{Ca}^{2+}$ -ATPase inhibition. As shown in Table 3, the  $k_2/k_1$  values in the presence of MgADP were constant for C<sub>0</sub>, C<sub>3</sub>, and C<sub>6</sub> but increased significantly for C<sub>7</sub>, revealing a sudden change in behavior at this reagent length (Figure 5). The result was confirmed by the fact that a similar jump was observed for the corresponding experiments at pH 7. At the lower pH, even reagent C<sub>8</sub> could be used, showing that a further increase in cross-linking rate occurred between  $n = 7$  and  $n = 8$  (Figure 5).

A similar dependence of  $k_2/k_1$  was found in the absence of MgADP, suggesting that the distance between SH1 and SH2 is not changed when the nucleotide is added or removed (Figure 5). Thus we conclude that the distance between SH1 and SH2 is  $\geq 15$  Å under both conditions. The similarity of the values in the presence and absence of MgADP raises doubts about changes in the distance between SH1 and SH2 derived from previous studies (55, 56).

At present it is difficult to understand why C<sub>3</sub> and C<sub>6</sub> in the presence and absence of MgADP (and in the presence of MgADP even C<sub>0</sub>) allow cross-linking between SH1 and SH2 at all. In models, the two thiols are at a distance of ca. 17 Å and separated by helical structures (Figure 9). An approach of the two SH groups down to 2 Å would require an  $\alpha$ -helix-loop transition of this region, a process that can hardly be trapped by crystallography. Since most of the models studied by crystallography lacked the lever arm, it

was suggested that the helical structure might not exist in S1 containing the light chain binding region, an argument that was excluded by recent work of Cohen and co-workers (6). An important factor for the formation of cross-links with such short reagents is certainly the dynamic nature of proteins in solution. The so-called “breathing” effect might be expected to produce conformations that possess shorter distances between the two thiols and thus would allow cross-linking even with reagents distinctly shorter than 17 Å. In such a dynamic equilibrium SH1/SH2 conformations having a distance of  $\geq 15$  Å may be energetically favored, thus explaining the distance found in the crystal where the lowest energy conformation is frozen. The average value of  $\geq 15$  Å in solution as determined in this study may thus well correspond to the value of 17 Å as found in the crystals. On the other hand, it might be doubted that “breathing” alone is sufficient to explain such short-length bridging between these two thiols. Thus a melting process of the two helices may indeed occur, a possibility that has already been suggested by the work of Polosukhina and Highsmith (38).

**Reactivity of SH2.** In absence of nucleotide, cross-linking is generally ca. 15 times slower than in the presence of MgADP under otherwise equal conditions (Table 3). A possible explanation for this is that in rigor SH2 is buried or shielded, as already proposed (53, 57). A structure possibly shielding the thiol is loop 583–587, which according to Figure 9 (red spheres) would protect SH2 much more efficiently in the absence of MgADP than in the MgADP complex. Another possible shielding structure is again loop 501–518, which is associated with the switch-2 helix (Figure 9) forming in the absence of MgADP a steric hindrance exactly between SH2 and SH1 to which the cross-linking moiety is attached. As already mentioned, this loop is not visible in the X-ray structure of the MgADP complex; it may be flexible and thus allow better cross-linking than in the absence of the nucleotide.

## ACKNOWLEDGMENT

We thank Ken Holmes for continuous support of this work and helpful discussions. We also thank Gisela Helmig for kindly providing myosin, Jochen Reinstein for his help, especially with the kinetic analysis, John Wray for critical reading of the manuscript, Suse Zobeley for technical assistance, and the reviewers for valuable comments.

## REFERENCES

1. Rayment, I., Rypniewski, W. R., Schmidt-Bäse, K., Smith, R., Tomchick, D. R., Benning, M. M., Winkelmann, D. A., Wesenberg, G., and Holden, H. M. (1993) *Science* 261, 50–58.
2. Gulick, A. M., Bauer, C. D., Thoden, J. B., and Rayment, I. (1997) *Biochemistry* 36, 11619–11628.
3. Fisher, A. J., Smith, C. A., Thoden, J. B., Smith, R., Sutoh, K., Holden, H. M., and Rayment, I. (1995) *Biochemistry* 34, 8960–8972.
4. Smith, C. A., and Rayment, I. (1995) *Biochemistry* 34, 8973–8981.
5. Smith, C. A., and Rayment, I. (1996) *Biochemistry* 35, 5404–5417.
6. Dominguez, R., Freyzon, Y., Trybus, K. M., and Cohen, C. (1998) *Cell* 94, 559–571.
7. Holmes, K. C. (1997) *Curr. Biol.* 7, R112–R118.
8. Holmes, K. C. (1998) *Nat. Struct. Biol.* 11, 940–942.
9. Uyeda, T. Q. P., Abramson, P. D., and Spudich, J. A. (1996) *Proc. Natl. Acad. Sci. U.S.A.* 93, 4459–4464.
10. Kinose, F., Wang, S. X., Kidambi, U. S., Moncman, C. L., and Winkelmann, D. A. (1996) *J. Cell Biol.* 134, 895–909.
11. Suzuki, Y., Ohkura, R., Sugiura, S., Yasuda, R., Jr., K. K., Tanokura, M., and Sutoh, K. (1997) *Biochem. Biophys. Res. Commun.* 234, 701–706.
12. Patterson, B., Ruppel, K. M., Wu, Y., and Spudich, J. A. (1997) *J. Biol. Chem.* 272, 27612–27617.
13. Kielley, W. W., and Bradley, L. B. (1956) *J. Biol. Chem.* 208, 653–659.
14. Sekine, T., and Kielley, W. W. (1964) *Biochim. Biophys. Acta* 81, 336–345.
15. Yamaguchi, M., and Sekine, T. (1966) *J. Biochem. (Tokyo)* 59, 24–33.
16. Seidel, J. C. (1969) *Biochim. Biophys. Acta* 180, 216–219.
17. Reisler, E., Burke, M., and Harrington, W. F. (1974) *Biochemistry* 13, 2014–2022.
18. Burke, M., and Reisler, E. (1977) *Biochemistry* 16, 5559–5563.
19. Wells, J. A., Werber, M. M., and Yount, R. G. (1979) *Biochemistry* 18, 4800–4805.
20. Wells, J. A., Knoeber, C., Sheldon, M. C., Werber, M. M., and Yount, R. G. (1980) *J. Biol. Chem.* 255, 11135–11140.
21. Reisler, E., Burke, M., Himmelfarb, S., and Harrington, W. F. (1974) *Biochemistry* 13, 3837–3840.
22. Wells, J. A., and Yount, R. G. (1980) *Biochemistry* 19, 1711–1717.
23. Huston, E. E., Grammer, J. C., and Yount, R. G. (1988) *Biochemistry* 27, 8945–8952.
24. Wells, J. A., and Yount, R. G. (1979) *Proc. Natl. Acad. Sci. U.S.A.* 76, 4966–4970.
25. Wells, J. A., Sheldon, M., and Yount, R. G. (1980) *J. Biol. Chem.* 255, 1598–1602.
26. Miller, L., Coppedge, J., and Reisler, E. (1982) *Biochem. Biophys. Res. Commun.* 106, 117–122.
27. Nitao, L. K., and Reisler, E. (1998) *Biochemistry* 37, 16704–16710.
28. Margossian, S. S., and Lowey, S. (1982) *Methods Enzymol.* 85, 55–71.
29. Weeds, A. G., and Taylor, R. S. (1975) *Nature (London)* 257, 54–55.
30. Weeds, A. G., and Pope, B. (1977) *J. Mol. Biol.* 111, 129–145.
31. Wagner, P. D., and Weeds, A. G. (1977) *J. Mol. Biol.* 109, 445–473.
32. Bradford, M. M. (1976) *Anal. Biochem.* 72, 248–254.
33. Spudich, J. A., and Watt, J. (1971) *J. Biol. Chem.* 240, 4866–4871.
34. Houk, T. W., Jr., and Ue, K. (1974) *Anal. Biochem.* 62, 66–74.
35. Criddle, A. H., Geeves, M. A., and Jeffries, T. (1985) *Biochem. J.* 232, 343–349.
36. Riddles, P. W., Blakeley, R. L., and Zender, B. (1979) *Anal. Biochem.* 94, 75–81.
37. Kodama, T., Fukui, K., and Kometani, K. (1986) *J. Biochem.* 99, 1465–1472.
38. Polosukhina, K., and Highsmith, S. (1997) *Biochemistry* 36, 11952–11958.
39. Faulstich, H., Heintz, D., and Drewes, G. (1992) *FEBS Lett.* 302, 201–205.
40. Faulstich, H., and Heintz, D. (1995) *Methods Enzymol.* 251, 357–366.
41. *Organikum* (1990) 18th ed., pp 206–207, Deutscher Verlag der Wissenschaften, Berlin.
42. Sutoh, K. (1981) *Biochemistry* 20, 3281–3285.
43. Schägger, H., and von Jagow, G. (1987) *Anal. Biochem.* 166, 368–379.
44. Laemmli, U. K. (1970) *Nature* 227, 680–685.
45. Elzinga, M., and Collins, J. H. (1977) *Proc. Natl. Acad. Sci. U.S.A.* 74, 4281–4284.
46. Furch, M., Geeves, M. A., and Manstein, D. J. (1998) *Biochemistry* 37, 6317–6326.
47. Marston, S. B. (1982) *Biochem. J.* 203, 453–460.
48. Reichert, A., Heintz, D., Echner, H., Voelter, W., and Faulstich, H. (1996) *J. Biol. Chem.* 271, 1301–1308.
49. Mornet, D., Pantel, P., Audemard, E., and Kassab, R. (1979) *Biochem. Biophys. Res. Commun.* 89, 925–932.
50. Yamamoto, K., and Sekine, T. (1980) *J. Biochem. (Tokyo)* 87, 219–226.
51. Xie, L., and Schoenberg, M. (1998) *Biochemistry* 37, 8048–8053.
52. Phan, B. C., Peyser, Y. M., Reisler, E., and Muhlrad, A. (1997) *Eur. J. Biochem.* 243, 636–642.
53. Xing, J., and Cheung, H. C. (1995) *Biochemistry* 34, 6475–6487.
54. Hiratsuka, Y., Eto, M., Yazawa, M., and Morita, F. (1998) *J. Biochem. (Tokyo)* 124, 609–614.
55. Dalbey, R. E., Weiel, J., and Yount, R. G. (1983) *Biochemistry* 22, 4696–4706.
56. Cheung, H. C., Gonsoulin, F., and Garland, F. (1985) *Biochim. Biophys. Acta* 832, 52–62.
57. Hiratsuka, T. (1992) *J. Biol. Chem.* 267, 14941–14948.

BI990615C